Electronic Structure and Bonding in Tetradecker Sandwich Complexes†

Eluvathingal D. Jemmis* and A. Chandrasekhar Reddy

Contribution from the School of Chemistry, University of Hyderabad, Central University P.O., Hyderabad-500 134, India. *Received June 30, 1989*

Abstract: Electronic structure of tetradecker sandwich compounds, CpMCpM'CpMCp, have been studied by using the fragment moleular orbital approach within the extended Hückel molecular orbital theory. Forty-six valence electron complexes are found to have highly antibonding degenerate HOMOs which lead to a distorted structure where the two end CpMCp units slip away from the central metal in a direction perpendicular to the original metal-metal axis (**5**). The extent of antibonding interactions is maximum when the M' is a late transition metal and M is an early transition metal of the periodic table. With appropriate metals it is possible to have a symmetric 46 valence electron tetradecker complex. Calculations on a series of $CpCo(C_3B_2H_5)M'(C_3B_2H_5)CoCp$ where M' = Cr, Mn, Fe, Co, Ni, Cu, and Zn reproduced the experimental structural trends. The variation in total energies has been traced predominantly to the energy difference between the valence orbitals of the metal atoms and the π and σ MOs of the ring. Qualitative prediction of the extent of slipping is difficult because of the simultaneous variation of the number of valence electrons and the metal atom parameters. However calculations with appropriate atomic parameters reproduce the experimental trends well. The bent geometry of $CpCo(C_3B_2H_5)Sn(C_3B_2H_5)CoCp$ is caused by the factors similar to those that operate in making CpSnCp a bent metallocene.

The versatile chemistry of the metallocenes, **1**, has encouraged the study of the oligomers obtained by sandwiching additional metal-ring combinations. Addition of a metal and a ring to **1** leads to the triple-decker sandwiches, **2**, a popular topic of research.[1] The variations possible in the triple-decker sandwiches such as the metal, type of atoms involved in the ring and the ring size, presence or lack of metal-metal bonding, all indicate a rich chemistry lying ahead in the area. Many theoretical studies on these triple-decker sandwich compounds have been known.[2] Higher homologs and polymetallocenes[3]—one-dimensional stack of alternating metal and ring—provide exciting challenges.

Addition of one metal and ring to **2** leads to the tetradecker sandwiches, **3**, which are the subject of the present study. The

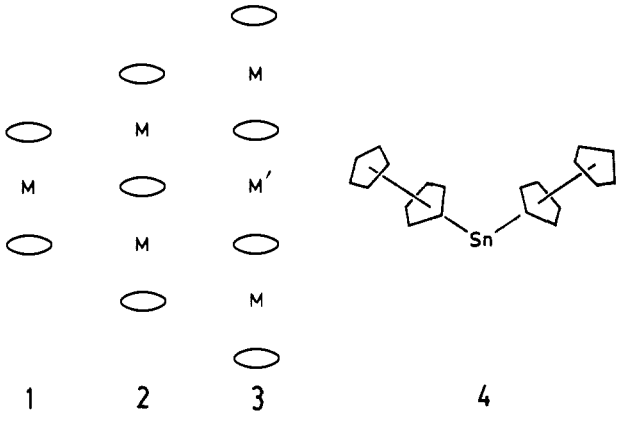

first tetradecker sandwich was synthesized only 10 years ago. Pioneering work of Siebert and co-workers led to the isolation and characterization of $[(C_2B_2SR_4)Co(C_2B_2SR_4)]_2Fe$.[4] A variety of tetradecker complexes followed with $C_3B_2H_5$ and its derivatives as ligands.[4-14] Table I lists the set of tetradecker complexes that have been characterized by diffraction methods. The number of valence electrons in these compounds varies from 40 to 46. There is also an isolated example of a complex having 48 valence electrons with Sn as the central metal, M'.[6] This forms a tetradecker structure where the two metallocene units sandwich the Sn at an angle of 112°, **4**. Another remarkable structural feature exhibited by some of the tetradecker sandwiches is the slip-distortion, **5**, seen in a series of complexes $CpCo(C_3B_2H_5)M'(C_3B_2H_5)CoCp$ (M = Cr-Zn) synthesized by the Siebert group.[8-10] Here the two terminal metallocenes slip away from the central metal M' by differing amounts. The extent of slipping varies with the central metal, M', and ranges from 0.1 to 0.5 Å (Table I). There is no obvious correlation between the magnitude of slipping and the number of valence electrons. A 46-electron Zn complex, $CpCo(C_3B_2H_5)Zn(C_3B_2H_5)CoCp$, has a slipping of 0.45 Å, but the Pt complex, $[CpNi(C_3B_2H_5)]_2Pt$, with the same electron count has no slipping at all. Theoretical studies on triple-decker sandwiches have shown that a general electronic structure description is not applicable to the whole set of complexes. The structural details of these complexes depend very much on the specific metals and the ligands involved. Tetradecker sandwiches should provide even greater variety. We study here the electronic structure of tetradecker sandwiches with a view to understand these structural variations. Our analysis begins with the electronic structure of a simple hypothetical tetradecker sandwich $CpCoCpCoCpCoCp^+$ with 46 valence electrons. Variations in the electronic structure with different rings and metals found experimentally were studied for a large set of complexes. The

† Dedicated to Professor Paul von Raguē Schleyer on the occasion of his 60th birthday.

(1) (a) Werner, H.; Salzer, A. *Synth. Inorg. Met.-Org. Chem.* **1972**, *2*, 239. (b) Beer, D. C.; Miller, V. R.; Sneddon, L. G.; Grimes, R. N.; Mathew, M.; Palenic, G. J. *J. Am. Chem. Soc.* **1973**, *95*, 3046. (c) Scherer, O. J.; Schwall, J.; Swarowsky, H.; Wolmershauser, G.; Kaim, W.; Gross, R. *Chem. Ber.* **1988**, *121*, 443. (d) See ref 1-16 in 2b. (e) Davis, J. H.; Sinn, E.; Grimes, R. N. *J. Am. Chem. Soc.* **1989**, *111*, 4776, 4784.

(2) Lauher, J. W.; Elian, M.; Summerville, R. H.; Hoffmann, R. *J. Am. Chem. Soc.* **1976**, *98*, 3219. (b) Jemmis, E. D.; Reddy, A. C. *Organometallics* **1988**, *7*, 1561. (c) Au-Chin, T.; Liquian-Shu *Int. J. Quantum Chem.* **1986**, *29*, 579. (d) Chesky, P. T.; Hall, M. B. *J. Am. Chem. Soc.* **1984**, *106*, 5186. (e) Tremel, W.; Hoffmann, R.; Kertesz, M. *J. Am. Chem. Soc.* **1989**, *111*, 2030.

(3) Kuhlmann, T.; Roth, S.; Roziere, J.; Siebert, W. *Angew. Chem.* **1986**, *98*, 88; *Angew. Chem., Int. Ed. Engl.* **1986**, *25*, 105.

(4) Siebert, W.; Rothermel, W.; Bohle, C.; Kruger, C.; Brauer, D. J. *Angew. Chem., Int. Ed. Engl.* **1979**, *18*, 949; *Angew. Chem.* **1979**, *91*, 1014.

(5) Siebert, W. *Angew. Chem.* **1985**, *97*, 924; *Angew. Chem., Int. Ed. Engl.* **1985**, *24*, 943.

(6) Wadepohl, H.; Pritzkow, H.; Siebert, W. *Organometallics* **1982**, *2*, 1899.

(7) (a) Grimes R. N. *Coord. Chem. Rev.* **1979**, *28*, 47. (b) Sandwich compounds of the general formula $CpCo(C_3B_2R_5)Co(C_2B_3R_5)M(C_nR_m)$ (where M = Co, Rh, Ru and n = 5, 6) are already synthesized. Grimes, R. N. Private communication.

(8) Siebert, W.; Edwin, J.; Wadepohl, H.; Pritzkow, H. *Angew. Chem., Int. Ed. Engl.* **1982**, *21*, 149; *Angew. Chem.* **1982**, *94*, 148.

(9) Edwin, J.; Bohm, M. C.; Chester, N.; Hoffman, D. M.; Hoffmann, R.; Pritzkow, H.; Siebert, W.; Stumpf, K.; Wadepohl, H. *Organometallics* **1983**, *2*, 1666.

(10) Wadepohl, H.; Dissertation Universitat Marburg, 1982.

(11) Siebert, W.; Bohle, C.; Kruger, C. *Angew. Chem., Int. Ed. Engl.* **1980**, *19*, 746; *Angew. Chem.* **1980**, *92*, 758.

(12) Edwin, J.; Bochmann, M.; Bohm, M. C.; Brennan, D. E.; Greiger, W. E.; Kruger, C.; Pebler, J.; Pritzkow, H.; Siebert, W.; Swiridoff, W.; Wadepohl, H.; Weiss, J.; Zenneck, U. *J. Am. Chem. Soc.* **1983**, *105*, 2582.

(13) Wadepohl, H.; Pritzkow, H.; Siebert, W. *Chem. Ber.* **1985**, *118*, 729.

(14) Herter, W.; Dissertation, Universitat Heidelberg, 1984.

0002-7863/90/1512-722$02.50/0

Table I. Geometric Parameters and Number of Valence Electrons of the Tetradecker Sandwich Compounds Characterized by Diffraction Methods

no.	compound	cp–M dist, Å	M–M dist, Å	no. of valence electrons	extent of slip-distortion	ref
I	$[(C_2B_2SR_4)Co(C_2B_2SR_4)]_2Fe$	1.69	3.53	42		4
II	$[(CpFe(C_2B_2SR_4)]_2M$					
	(a) M′ = Fe	1.67	3.27	42		11
	(b) M′ = Co	1.69	3.86	43		11
III	$(CpCo(C_3B_2R_5))_2M$					8–10
	(a) M′ = Cr	1.66	3.47	40	0.10	
	(b) M′ = Mn	1.66	3.53	41	0.20	
	(c) M′ = Fe	1.66	3.42	42	0.22	
	(d) M′ = Co	1.66	3.38	43	0.20	
	(e) M′ = Ni	1.66	3.28	44	0.10	
	(f) M′ = Cu	1.66	3.41	45	0.50	
	(g) M′ = Zn	1.66	3.46	46	0.45	
IV	$[CpNi(C_3B_2R_5)]_2Ni$			46		14
V	$[CpM(C_3B_2R_5)]_2Pt$					
	(a) M = Fe	1.66	3.40	42	0.00	13
	(b) M = Ni	1.66	3.59	46	0.00	13
VI	$[CpCo(C_2B_3R_5)]_2Co–H$			42	0.00	7
VII	$[CpCo(C_3B_2R_5)]_2Sn$[a]		1.66	48		6

[a] The two $[CpCoC_3B_2R_5)]$ units are bent by 112°.

origins of these variations were traced by fragment molecular orbital studies.[15] Variations in the metals that might allow the bent structures such as **4** were also examined. All calculations were carried out with the extended Hückel method[16] with geometries and parameters specified in the Appendix. Wherever possible structural parameters available from diffraction studies have been used in the calculations.

Results and Discussion

Electronic Structure of the Model Tetradecker Sandwich Complex $CpCoCpCoCpCoCp^+$ (6, M = M′ = Co). $CpCoCpCoCpCoCp^+$, **6**, with 46 valence electrons was selected

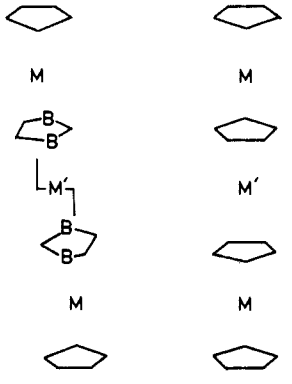

5 **6**

as a prototype of the tetradecker sandwiches for the initial set of calculations. The electronic structure of the model is constructed by interacting a central $CpCoCp^-$ unit with $CpCo^+$ groups from each side. The MOs of CpM′Cp are well-known.[17] However, an interaction diagram leading to the energy levels of $CpCoCp^-$ is given in Figure 1 to help in understanding the changes in the energy levels and in the MOs of the metallocenes, with different metals. The important MOs of the $CpCoCp^-$ involved in the tetradecker sandwich formation are $2e_{1g}$, $2e_{1u}$, and $3e_{1g}$. Of these, the $2e_{1u}$ orbitals are purely based on the ligands and could strongly interact with the MOs of the CpCo···CoCp group. The $3e_{1g}$ of $CpCoCp^-$ is the "e_g" equivalent of the octahedral complex. The $2e_{1g}$ is the corresponding ligand–metal bonding combination. The MOs of the fragment $CpCo···CoCp^{2+}$ are obtained from the monomer units $CpCo^+$ (Figure 2, left). The frontier orbitals of

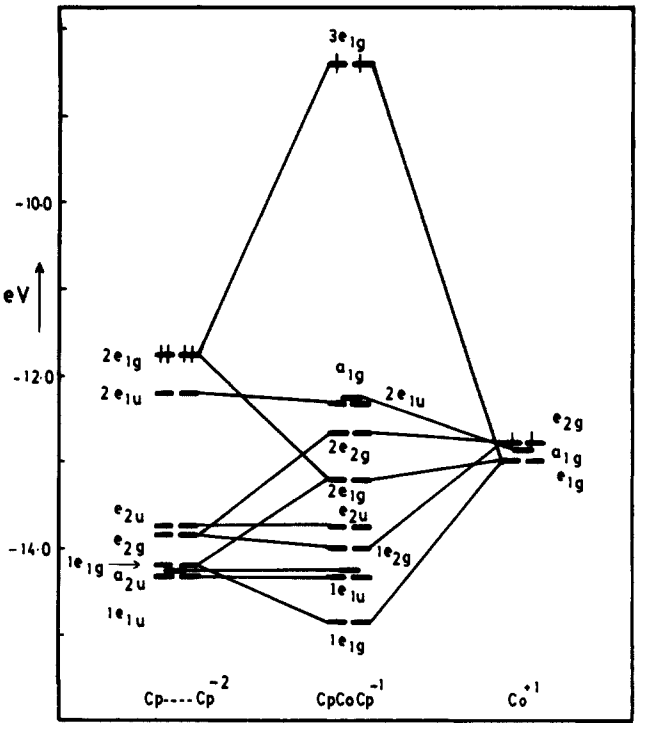

Figure 1. Construction of the orbitals of $CpCoCp^-$ from the fragments $Cp···Cp^{2-}$ and Co^+. Symmetry labels are for D_{5d} point group.

$CpCo^+$ are well-known. The nondegenerate MO from the "two below one" pattern of CpM is too high in energy to be of any consequence in bonding to $CpCoCp^-$. The degenerate MO of CpM forms the linear combinations of $2e_{1g}$ and $2e_{1u}$ of CpCo···$CoCp^{2+}$. The lower lying ligand based MOs le_{1g} and le_{1u} as seen below also influence the bonding between central metallocene and terminal metal.

The interaction diagram involving $CpCo···CoCp^{2+}$ and $CpCoCp^-$ is given in Figure 2 (middle). Several weak two-orbital four-electron interactions involving a_{1g}, a_{2u}, and e_{2g} MOs are not shown. The interaction leads to two e_{1u} pairs (le_{1u}, $2e_{1u}$) which are low in energy and filled. The antibonding combination, $3e_{1u}$, is vacant. The e_{1g} MOs also lead to two low-energy pairs; however, the third one, $3e_{1g}$, which is antibonding between the central metal and the adjacent rings, lies below $3e_{1u}$ and is filled in the 46 valence electron systems. The antibonding nature of $3e_{1g}$ is seen in **7**. Therefore, tetradecker systems with 42 valence electrons where the antibonding MOs are empty will be preferred. However, Table I shows that compounds with higher electron counts are known. There are three complexes reported with 46 valence electrons. Two

(15) (a) Fujimoto, H.; Hoffmann, R. *J. Phys. Chem.* **1974**, *78*, 1169. (b) Hoffmann, R.; Swenson, J. R.; Wan, C.-C. *J. Am. Chem. Soc.* **1973**, *95*, 7644.
(16) (a) Hoffmann, R. *J. Chem. Phys.* **1963**, *39*, 1397. (b) Hoffmann, R.; Lipscomb, W. N. *Ibid.* **1962**, *36*, 3179, 3489.
(17) Cotton, F. A. *Chemical Applications of Group Theory*, 2nd ed.; 1971; p 235.

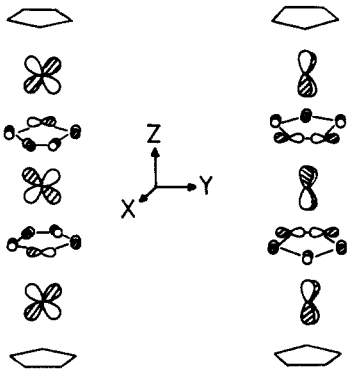

7a 7b

of these have been structurally characterized. Surprisingly, one of them, $CpCo(C_3B_2H_5)Zn(C_3B_2H_5)CoCp$, has a distorted structure, **5**, with a 0.45 Å slip of the terminal metallocene units with respect to the central metal, while the other, $CpNi(C_3B_2H_5)Pt(C_3B_2H_5)NiCp$, is almost symmetric along the metal axis. What are the causes for the structural differences in the 46 valence electron systems such as IIIg and Vb of Table I? Let us look at them closely. The terminal rings in both the complexes are cyclopentadienyls. The middle rings involve $C_3B_2H_5$ units albeit with different substituents. The only major difference is in the metals involved. Thus the CoZnCo combination in IIIg (Table I) is replaced by the NiPtNi combination in Vb (Table I) which retains the number of valence electrons. There seems to be no overriding packing effect that operates only in one and not in the other.

To understand the reasons for the distortions in the 46 valence electron systems in detail, a Walsh diagram is constructed for the distortion by moving the two terminal CpCoCp units away from each other along an axis perpendicular to the initial M–M axis (Figure 3). The degenerate HOMO, $3e_{1g}$, which is antibonding between the central metal and the adjacent rings, decreases in energy with distortion. Since the slipping is in the *yz* plane, the decrease in the M′–ring overlap and the antibonding interaction is more dramatic with the MO involving the d_{xz} orbital of the central metal, **7b** than **7a**. In this model compound the variation in the $3e_{1g}$ MOs almost parallel the behavior of the sum of one-electron energy. This leads to the immediate conclusion that all 46 valence electron tetradecker complexes should distort, contrary to the experimental observations. Scheme I gives how the $3e_{1g}$ orbitals are obtained from the $2e_{1g}$ and $3e_{1g}$ MOs of CpM′Cp and $2e_{1g}$ of CpM···MCp (Figure 2). The $2e_{1g}$ and $3e_{1g}$ MOs of CpM′Cp results from the combination of xz[18] and *yz* orbitals of M′ and $1e_{1g}$ and $2e_{1g}$ orbitals of Cp···Cp (Figure 1). $1e_{1g}$ orbitals of Cp···Cp is purely σ inplane orbitals of the Cp ring, whereas the $2e_{1g}$ orbitals of Cp···Cp are purely π orbitals. $3e_{1g}$ of CpM′Cp is pure π antibonding orbital between the metal, M′, and the Cp rings. The $2e_{1g}$ MOs of CpM′Cp changes with the metal M′. The extremes where the Cp contribution changes from π to σ are shown in Scheme I. Table II gives the coefficients of the p_z orbital of the carbon atoms in the $2e_{1g}$ orbital of CpM′Cp (M′ = Cr–Ni).

The extent of ring character of $3e_{1g}$ MOs of **6** depends on the magnitude and nature of the $2e_{1g}$ and $3e_{1g}$ MOs of CpM′Cp that constitute it. This is controlled by the energy difference between the $2e_{1g}$ MOs of CpM···MCp and the $2e_{1g}$ and $3e_{1g}$ MOs of CpM′Cp. Figure 4 gives the variation in the energies of the $2e_{1g}$ and $3e_{1g}$ orbitals of CpM′Cp (M′ = Cr–Ni) and those of the $2e_{1g}$ orbitals of CpM···MCp (M = Cr–Ni) fragment. The general expectation, that the energy levels go down with the increasing atomic number of the metal concerned, holds true.

Consider the CpCr···CrCp fragment interacting with the different metallocenes, CpM′Cp (M′ = Cr–Ni). The energy difference between the $3e_{1g}$ orbitals of CpM′Cp and the $2e_{1g}$ orbitals of CpCr···CrCp decreases in going from M′ = Cr to M′ = Ni. This also increases the energy difference between the $2e_{1g}$ orbital of CpM′Cp and the $2e_{1g}$ orbitals of CpCr···CrCp (Figure 4).

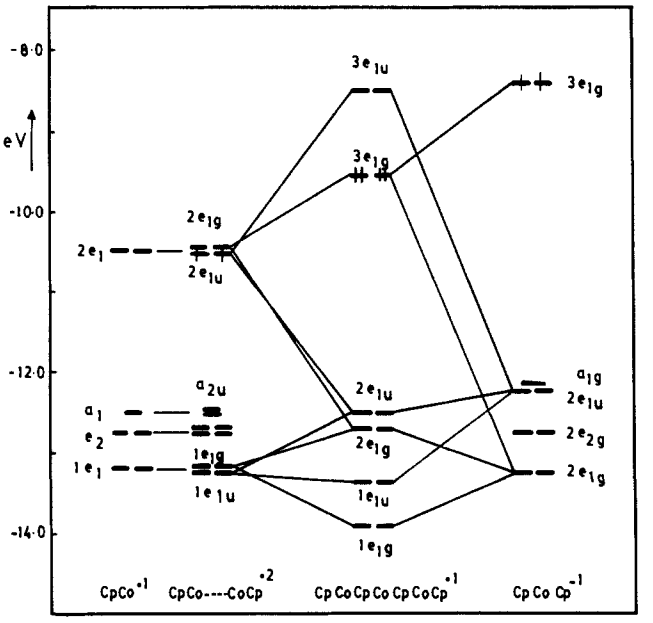

Figure 2. Construction of the orbitals of $CpCoCpCoCpCoCp^+$ from the fragments $CpCo\cdots CoCp^{2+}$ and $CpCoCp^-$. Several 4e – 2 orbital interactions are neglected in this.

Table II. Cp Ring p_z Orbital Coefficients of $2e_{1g}$ Orbital of CpM′Cp (M′ = Cr, Fe and Ni)

		MO coefficients				
no.	compound	C1	C2	C3	C4	C5
1	CpCrCp	0.1147	0.3324	0.0907	0.2764	0.2615
2	CpFeCp	0.1034	0.2892	0.0753	0.2426	0.2253
3	CpNiCp	0.0805	0.2142	0.0518	0.1821	0.1644

Table III

	M′		
M	Cr	Fe	Ni
Cr	a1	a2	a3
Fe	b1	b2	b3
Ni	c1	c2	c3

Decrease in the energy difference between the $3e_{1g}$ of CpM′Cp and $2e_{1g}$ of CpCr···CrCp enhances the interaction between them and leads to a $3e_{1g}$ pair that is strongly antibonding between M′ and adjacent rings. Increased antibonding interaction in $3e_{1g}$ leads to increased slip-distortion. On the other hand, the energy difference between the $2e_{1g}$ orbital of CpNi···NiCp and $3e_{1g}$ of CpCrCp is more compared with the $2e_{1g}$ orbital of CpNi···NiCp and $2e_{1g}$ orbital of CpCrCp. Therefore the contribution to the $3e_{1g}$ orbital of **6** is more from the $2e_{1g}$ of CpM′Cp compared with $3e_{1g}$ of CpM′Cp. Since $2e_{1g}$ orbital of CpM′Cp is a mixture of π and σ orbitals of Cp rings, larger contribution from this $2e_{1g}$ orbital to the $3e_{1g}$ of **6** leads to the increased σ character to the interaction between the central metal and the adjacent rings in the $3e_{1g}$ orbital. This results in decreased M′–ring interactions in $3e_{1g}$ MOs and less slipping. When M′ = Ni, a total reversal of the trend is observed.

To demonstrate these we have calculated potential energy surfaces for slipping in nine combinations of terminal and central metals in **6**, always keeping a 46 valence electron count by adding appropriate charges. The variations in the sum of one electron energies as a function of distortion is given in Figure 5. The nomenclature used to represent various combinations is given in Table III. Here the letters a, b, and c correspond to the terminal metals (M), while 1, 2, and 3 correspond to the central metal (M′), respectively. Thus a3 represents CpCrCpNiCpCrCp with appropriate charge to have 46 valence electrons. In Figure 5 the relative energies are adjusted uniformly to be zero at the symmetric structure. According to the discussion above, maximum decrease in energy by slipping should be for the CrNiCr combination a3

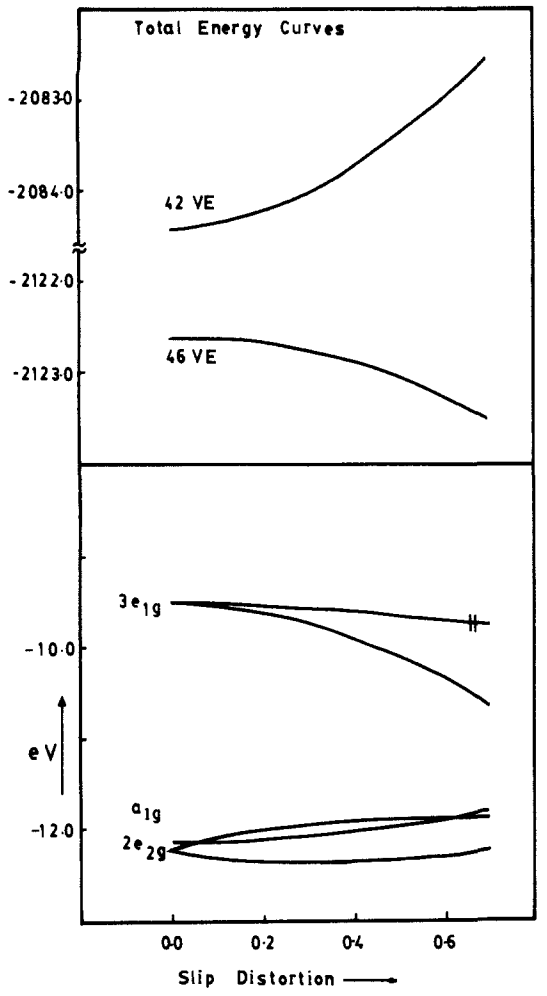

Figure 3. Walsh diagram for the slip distortion as observed in the 46 valence electron tetradecker sandwich compounds, **5**, with the model $CpCoCpCoCpCoCp^+$ (below). Sum of one-electron energies of 42 VE (valence electrons) and 46 VE complexes are given on the top half of the diagram.

Table IV. Fragment Orbital Contribution to the $3e_{1g}$ Orbital of CpMCpM'CpMCp

no.	CpMCpM'CpMCp	I fragment CpM···MCp $2e_{1g}$	II fragment CpM'Cp $3e_{1g}$	II fragment CpM'Cp $2e_{1g}$
1	M = Cr, M' = Cr	0.67	0.64	0.40
2	M = Cr, M' = Fe	0.58	0.72	0.35
3	M = Cr, M' = Ni	0.40	0.83	0.27
4	M = Fe, M' = Cr	0.76	0.49	0.46
5	M = Fe, M' = Fe	0.69	0.60	0.41
6	M = Fe, M' = Ni	0.49	0.78	0.28
7	M = Ni, M' = Cr	0.82	0.22	0.55
8	M = Ni, M' = Fe	0.82	0.29	0.51
9	M = Ni, M' = Ni	0.72	0.54	0.40
10	M = Co, M' = Co	0.67	0.58	0.41

which is indeed found to be the case (Figure 5). Table IV shows that in a3 the contribution to the $3e_{1g}$ orbitals of **6** from the $3e_{1g}$ orbitals of CpM'Cp is more (0.83) compared to that from the $2e_{1g}$ (0.27) orbital of CpM'Cp. In NiCrNi combination, c1, the contribution is more from the $2e_{1g}$ orbital (0.55) of CpM'Cp which gives more σ character to the ring contributions compared with the $3e_{1g}$ orbitals (0.22) giving less antibonding in the $3e_{1g}$ orbitals of **6**. Calculations show that the energy of the NiCrNi combination indeed goes up on distortion, Figure 5. The all-Ni combination, c3, changes very little in energy on distortion. b1, b2, and b3 fall approximately between a1, a2, a3 and c1, c2, c3 combinations. Thus a clear generalization for 46 valence electron tetradecker sandwiches follows: extent of slipping from the

Scheme I

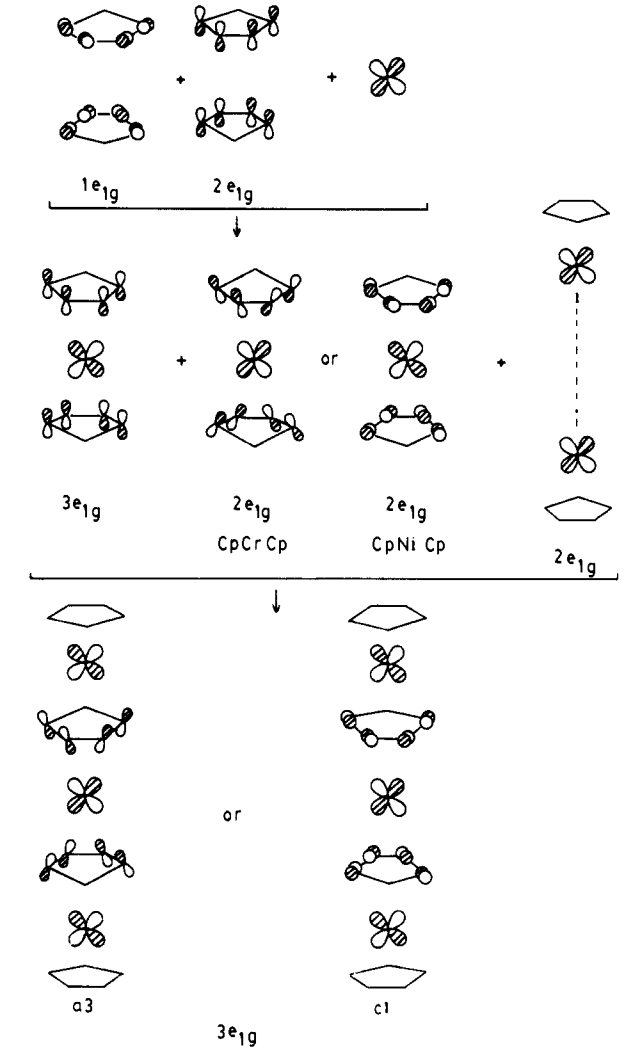

symmetric structure is maximum with M = early transition metal and M' = late transition metal (a3). Possibility of a slipped structure is minimum when the situation is reversed (c1).

Most of the experimentally known tetradecker complexes have $C_3B_2H_5$ and its derivatives as middle rings. Are the calculations obtained by using Cp rings relevant to these systems as well? A comparison between the $2e_{1g}$ and $3e_{1g}$ orbitals of CpCoCp and $(C_3B_2H_5)Co(C_3B_2H_5)$ reveals the following (Figure 4). $1e_{1g}$ and $2e_{1g}$ orbitals of $(C_3B_2H_5)$···$(C_3B_2H_5)$ lie higher in energy compared with those of Cp···Cp. This leads to more ligand character in the $3e_{1g}$ orbitals of $(C_3B_2H_5)M'(C_3B_2H_5)$ compared with those of CpM'Cp. Interaction of these $3e_{1g}$ orbitals with the $2e_{1g}$ orbitals of CpCo···CoCp results in strongly antibonding $3e_{1g}$ MOs of **6**. A direct comparison between $CpCoCpCoCpCoCp^+$ and $CpCo(C_3B_2H_5)Co(C_3B_2H_5)CoCp^{3-}$ with regard to the variation in total energy for slipping shows that the decrease in the sum of one-electron energies as a function of slipping is less for the all-Cp compound (Figure 6, d vs j).

Similar calculations were also carried out for the series of $CpCo(C_3B_2H_5)M'(C_3B_2H_5)CoCp$ (M' = Cr–Zn, a–g in Figure 6) with different charges so that 46 valence electrons are maintained. It is seen that the decrease in energy for the same extent of slipping increases initially in going from Cr to Ni and then decreases in the Cu and Zn complexes. The energy of the $3e_{1g}$ orbitals of $(C_3B_2H_5)M'(C_3B_2H_5)$ decreases gradually and becomes comparable to that of the $2e_{1g}$ MOs of CpM···MCp at M' = Ni. Further decrease in energy of M' (as in Cu and Zn) increases this energy difference so that the ring–M' interactions are not as strong. Correspondingly the $3e_{1g}$ orbital is less antibonding, resulting in less distortions. The foregoing discussions can be directly used in the two 46 valence electron count tetradecker complexes IIIg

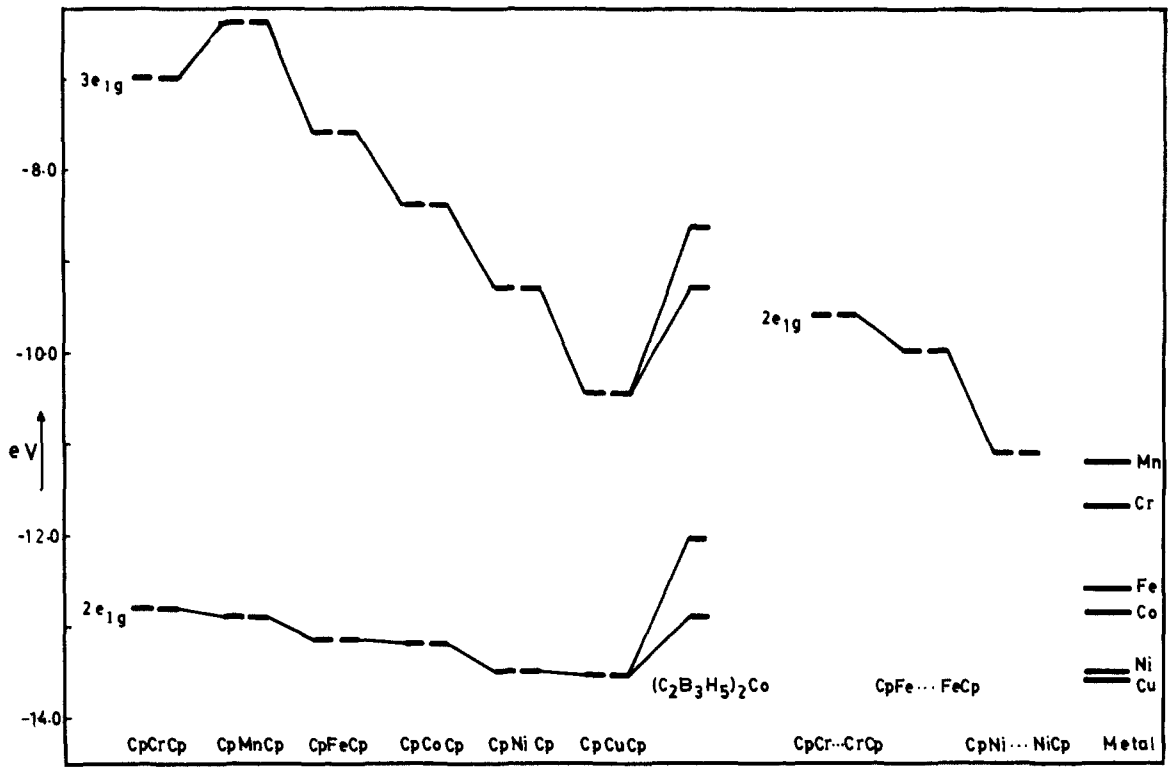

Figure 4. Correlation of the $2e_{1g}$ and $3e_{1g}$ levels of the metallocenes CpM'Cp (M' = Cr–Ni) (left) and the $2e_{1g}$ levels of CpM···MCp (M = Cr, Fe, Ni) fragments (middle). Metal d orbital energies are given on the right side.

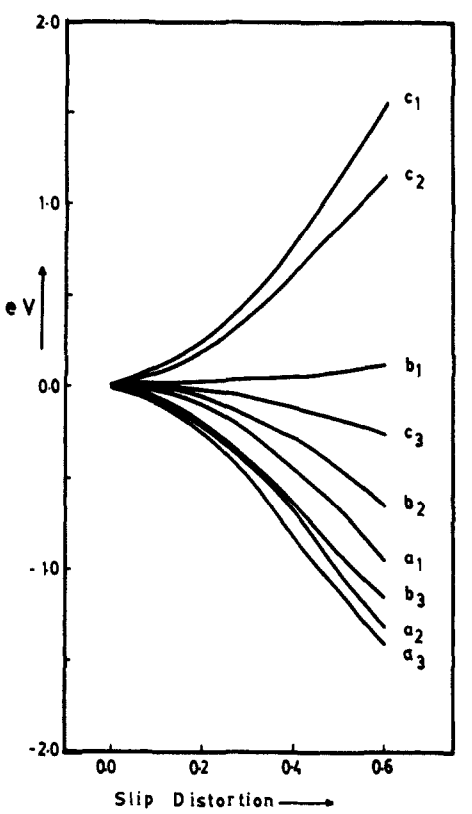

Figure 5. Plot of the sum of one-electron energies as a function of slip-distortion for 46 valence electron complexes of the type CpMCpM'CpMCp$^+$. (a1) M = Cr, M' = Cr; (a2) M = Cr, M' = Fe; (a3) M = Cr, M' = Ni; (b1) M = Fe, M' = Cr; (b2) M = Fe, M' = Fe; (b3) M = Fe, M' = Ni; (c1) M = Ni, M' = Cr; (c2) M = Ni, M' = Fe; (c3) M = Ni, M' = Ni. See Table III for explanations of a1, a2, etc.

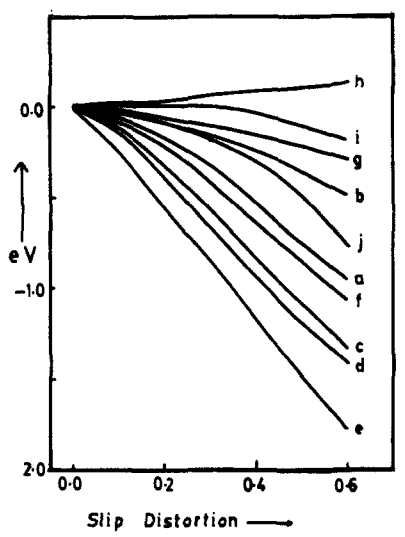

Figure 6. Plot of the sum of one-electrn energies as a function of slip-distortion for the complexes of the type CpCo($C_3B_2H_5$)M'($C_3B_2H_5$)CoCp (M' = Cr–Cu). Number of valence electrons in all the complexes is kept at 46: (a) M' = Cr; (b) M' = Mn; (c) M' = Fe; (d) M' = Co; (e) M' = Ni; (f) M' = Cu; (g) M' = Zn; (h) (CpNi$C_3B_2H_5$)$_2$Pt; (i) (CpNi$C_3B_2H_5$)$_2$Ni; (j) CpCoCpCoCpCoCp$^+$.

and Vb of Table I. The terminal metal M has gone from Co in IIIg to Ni in Vb which leads to less p_z character on the $C_3B_2H_5$ ligands in the $3e_{1g}$ orbitals. Similarly the change of the central metal from Zn to Pt also decreases the tendency for slipping according to the discussion above. The variation of energy with slip distortion for the NiPtNi combination is given in Figure 6 (curve h) which shows that the energy *increases* though not very steeply with distortion. Thus the general conclusions about slipping hold good. This also helps us to predict the structure of CpNi($C_3B_2H_5$)Ni($C_3B_2H_5$)NiCp which is known experimentally, but no structural studies are available. The difference between Vb and the NiNiNi complex is that the central metal is changed from Pt to Ni. Thus the tendency for distortion should be very low in this complex (Figure 6, curve i). The most important conclusion to be drawn from the above discussion is that all 46 valence electron tetradecker complexes need not have a slipped structure. Qualitative trends can be obtained for the relation between M and M' and the extent of distortion.

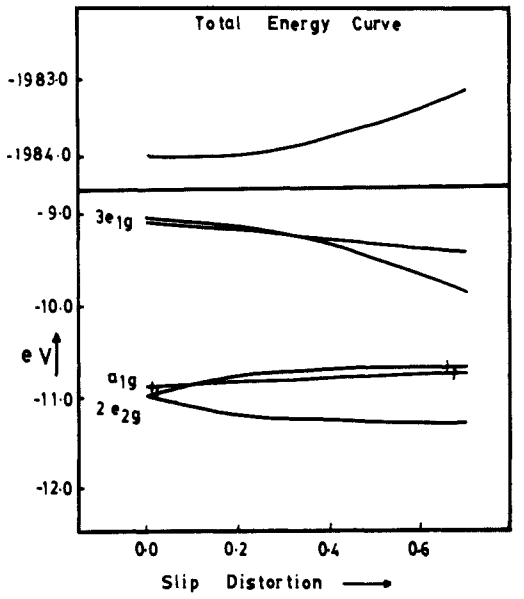

Figure 7. Walsh diagrams for the slip-distortion observed in the tetradecker sandwich compound $CpCo(C_3B_2H_5)Cr(C_3B_2H_5)CoCp$ as a representative of tetradecker complexes with $C_3B_2H_5$ middle rings. Variation of the sum of one-electron energies of this 40 VE complex is given on the top.

The complexity involved in understanding the slip-distortions in tetradecker sandwiches are obvious: even with 46 valence electrons the extent of distortion should vary considerably. Simultaneous changes in the number of valence electrons and the central metal make predictions difficult in the series IIIa–g (Table I). However, we find that extended Hückel calculations with a standard set of parameters for each metal is able to reproduce the trends correctly. A representative example, the 40 valence electron complex $CpCo(C_3B_2H_5)Cr(C_3B_2H_5)CoCp$, will be discussed first. Figure 7 gives a Walsh diagram as well as variation of one-electron energies for distortion. The general pattern of the MOs is similar to that in the all Cp analogue. There are only 40 valence electrons in this Cr complex so that the antibonding MOs, $3e_{1g}$, are empty. Thus the cause of the major distortion is absent. Sum of one-electron energies calculated for the Cr complex, assuming an occupancy $(2e_{1g})^4$, $(2e_{1u})^4$, $(2e_{2g})^3$, $(a_{1g})^1$, and $(3e_{1g})^0$, showed a minimum between 0.1 and 0.2 Å distortion close to the experimental value of 0.1 Å (Table I). Similar calculations with appropriate occupancy of levels for the remaining complexes in the series gave energy minima close to the experimental distances. The variations in the energy can be traced to the unsymmetrical nature of the $C_3B_2H_5$ ligands. Small distortions have been previously noted in transition-metal complexes[19] with unsymmetrical π ligands.

There is also a parallel, as noted earlier,[5] between the M′–ring distance and the extent of distortion. As the antibonding MOs are occupied there are only a few options for the complex to reduce the antibonding interactions. One is to increase the M′–ring distance. The other is to distort the geometry to a slipped structure **5**. Both are operative. The best mix of these two is adapted in each case, leading to a rough parallel between the M′–ring distance and the extent of slip-distortion.

The only example of a bent tetradecker complex, **4**, is found with the central metal Sn. The electronic structure of $(CpCo(C_3B_2H_5))_2Sn$ differs from the transition-metal tetradecker complexes in the following way. The 4d orbitals of Sn are too low in energy to interact with the MOs of $(CpCo(C_3B_2H_5))_2$. The a_{1g}, a_{2u}, and $3e_{1u}$ orbitals of $(CpCoC_3B_2H_5)_2$ has the right symmetry to interact with the 5s, $5p_z$ and $5p_x$, p_y orbitals of Sn, respectively. These interactions are very weak with M′ = transition metal. When M′ = Sn, these are the only interactions that bind the metallocene to Sn. We constructed a Walsh diagram for the bending of $(CpCoC_3B_2H_5)_2Sn$ so as to give the structure **4**. The decrease in the energy of $2a_{1g}$ MO is mainly responsible for the observed bending. The sum of one-electron energy gave a minimum around 120° of bending. The reason for bending is the same as that found for bending in the Cp_2Sn[20] and is not discussed further.

Conclusions

Extended Hückel molecular orbital studies on a large set of tetradecker complexes of the type CpMCpM′CpMCp (M = Cr–Ni, M′ = Cr–Ni) and $CpMC_3B_2H_5M'C_3B_2H_5MCp$ (M = Co, Ni and M′ = Cr–Zn) revealed the following. Forty-six valence electron count demands that four electrons have to occupy the antibonding MOs. These complexes distort from the high symmetry to reduce the antibonding interactions. The nature of the metal and the ligands decide the extent of antibonding interaction in the HOMO $(3e_{1g})$ of the 46 electron systems. Calculations on the 46 valence electron systems of the type CpMCpM′CpMCp shows that the extent of slipping from the symmetrical structure is maximum with M = early transition metal and M′ = late transition metal (Figure 5, a3). Possibility of a slipped structure is minimum when the situation is reversed (Figure 5, c1). A comparison between $CpCoCpCoCpCoCp^+$ and $CpCo(C_3B_2H_5)Co(C_3B_2H_5)CoCp^{3-}$ with regard to the variation in total energy for slipping shows that the decrease in sum of one-electron energies as a function of slip-distortion is less for the complex $CpCoCpCoCpCoCp^+$. There is no slipping of the metallocene units around the central metal in the tetradecker complexes Cp_4M_3 with 42 or less valence electrons. Small amounts of slip-distortions found in the complexes with $C_3B_2H_5$ as middle rings having 42 or less valence electron systems is attributed to the unsymmetrical nature of these rings. The decrease in energy of the a_{1g} orbital is responsible for the observed bending in $CpCo(C_3B_2H_5)Sn(C_3B_2H_5)CoCp$.

Acknowledgment. We thank the computational facilities of the National Informatic Centre and of the University of Hyderabad for computations. A.C.R. thanks the Council of Scientific and Industrial Research, New Delhi, for financial assistance.

Appendix

Atomic parameters for all the atoms used in the calculations are taken from previous studies.[21] Geometrical parameters are taken from the experimental structures wherever known (Table I). All C–C, C–H, C–B, B–H, and Cp ring center–M distances used in the calculations are 1.40, 1.08, 1.55, 1.21, and 1.66 Å, respectively.

(18) Throughout this paper coordinates xz and yz, etc. are used to indicate d orbitals d_{xz} and d_{yz}, etc.

(19) (a) Albright, T. A.; Hoffmann, R. *Chem. Ber.* **1978**, *111*, 1578. (b) Cox, D. N.; Mingos, D. M. P.; Hoffmann, R. *J. Chem. Soc., Dalton Trans.* **1981**, 1788.

(20) (a) Jutzi, P.; Kohl, F.; Hofmann, P.; Kruger, C.; Tsay, Y.-H. *Chem. Ber.* **1980**, *113*, 757. (b) Jutzi, P. *Adv. Organometallic Chem.* **1986**, *26*, 217.

(21) (a) Hoffman, D. M.; Hoffmann, R.; Fisel, C. R. *J. Am. Chem. Soc.* **1982**, *104*, 3858. (b) Chu, San-Yan; Hoffmann, R. *J. Phys. Chem.* **1982**, *86*, 1289. (c) Mehrotra, P. K.; Hoffmann, R. *Inorg. Chem.* **1978**, *17*, 2187. (d) Cox, D. N.; Mingos, D. M. P.; Hoffmann, R. *J. Chem. Soc., Dalton Trans.* **1981**, 1788. (e) Tremel, W.; Hoffmann, R. *Inorg. Chem.* **1987**, *26*, 118.